Development 125, 4739-4748 (1998)
Printed in Great Britain © The Company of Biologists Limited 1998
DEV1289



# *Hoxa1* and *Krox-20* synergize to control the development of rhombomere 3

**Françoise Helmbacher[1], Cristina Pujades[1], Carole Desmarquet[1], Monique Frain[1], Filippo M. Rijli[2], Pierre Chambon[2] and Patrick Charnay[1,*]**

[1]Unité 368 de l'Institut National de la Santé et de la Recherche Médicale, Ecole Normale Supérieure, 46 rue d'Ulm, 75230 Paris Cedex 05, France
[2]Institut de Génétique et de Biologie Moléculaire et Cellulaire, CNRS/INSERM/Université Louis Pasteur/Collège de France, BP 163, 67404, Illkirch Cedex, France
*Author for correspondence (e-mail: charnay@wotan.ens.fr)

*Accepted 11 September; published on WWW 9 November 1998*

## SUMMARY

**The transcription factor genes *Hoxa1* and *Krox-20* have been shown to play important roles in vertebrate hindbrain segmentation. In this report, we present evidence for novel functions of these genes which co-operate in specifying cellular identity in rhombomere (r) 3. Although *Hoxa1* has not been observed to be expressed rostrally to the prospective r3/r4 boundary, its inactivation results in (i) the appearance of patches of cells presenting an r2-like molecular identity within r3, (ii) early neuronal differentiation in r3, normally characteristic of even-numbered rhombomeres, and (iii) abnormal navigation of r3 motor axons, similar to that observed in even-numbered rhombomeres. These phenotypic manifestations become more severe in the context of the additional inactivation of one allele of the *Krox-20* gene, demonstrating that *Hoxa1* and *Krox-20* synergize in a dosage-dependent manner to specify r3 identity and odd- versus even-numbered rhombomere characters. In addition, these data suggest that the control of the development of r3 may not be autonomous but dependent on interactions with *Hoxa1*-expressing cells.**

Key words: Hindbrain, Krox-20, Hox genes, Rhombomere, Genetic interaction, Gene regulation, Neurogenesis, Cell segregation

## INTRODUCTION

The regionalisation of the vertebrate hindbrain along the anteroposterior axis involves a highly evolutionarily conserved segmentation process, which leads to the generation of a series of 7-8 lineage-restricted cellular compartments, called rhombomeres (r) (Lumsden and Keynes, 1989; Fraser et al., 1990; Birgbauer and Fraser, 1994; Lumsden and Krumlauf, 1996; Wingate and Lumsden, 1996; Schneider-Maunoury et al., 1998). This subdivision plays an essential role in establishing the pattern of both hindbrain and craniofacial (branchial) morphogenesis. In particular, it presages the periodic organisation of neurons (Lumsden and Keynes, 1989; Clarke and Lumsden, 1993) and correlates with the pathways of neural crest migration into the branchial arches (Lumsden and Guthrie, 1991; Lumsden et al., 1991; Serbedzija et al., 1992; Birgbauer et al., 1995; Köntges and Lumsden, 1996). The restriction in cell mixing between adjacent rhombomeres is thought to allow each segment to maintain a specific pattern of gene expression and a distinct rostrocaudal identity.

A number of putative regulatory genes have been shown to present spatially restricted patterns of expression along the anteroposterior axis in the hindbrain, with limits corresponding to prospective or established rhombomere boundaries (reviewed in Lumsden and Krumlauf, 1996). Mutational analyses indicate that several of these genes indeed play essential roles in the control of hindbrain development (reviewed in Schneider-Maunoury et al., 1998). The associated phenotypes observed to date fall into three classes. Several genes are required for the maintenance and/or generation of specific hindbrain territories: *Hoxa1* for parts of r4 and r5 (Chisaka et al., 1992; Lufkin et al., 1991; Carpenter et al., 1993; Dollé et al., 1993; Mark et al., 1993), *Krox-20* for r3 and r5 (Schneider-Maunoury et al., 1993, 1997; Swiatek et al., 1993) and *kreisler* for r5 and r6 (Cordes and Barsh, 1994; Frohman et al., 1993; McKay et al., 1994). A second category of genes, which so far only includes *Hox* genes, has been demonstrated to contribute to the specification of the positional identity of particular rhombomeres (Zhang et al., 1994; Alexandre et al., 1996; Studer et al., 1996; Gavalas et al., 1997). The involvement of a single gene in both processes also appears to be possible as suggested by loss-of-function and gain-of-function mutations of *Hoxa1*, which exhibit segmentation and homeotic phenotypes, respectively. Finally, members of the Eph family of transmembrane tyrosine kinase receptors and their ligands have been implicated in the segregation of cells between different rhombomeres (Xu et al., 1995).

Considering the essential role of these genes in the control of hindbrain development, it is becoming increasingly important to understand the relationships that might exist between them, both in terms of hierarchic organisation and of redundant or synergistic functions. During the past few years, several regulatory links have been revealed. The expression of

*Hoxb2* in r4 has been shown to be regulated by Hoxb1 (Maconochie et al., 1997) and autoregulatory loops have been demonstrated to play important roles in the transcription of *Hox* genes (Popperl et al., 1995; Gould et al., 1997). Krox-20 has been shown to control directly the transcription of *Hoxa2*, *Hoxb2* and *EphA4* in r3 and r5 (Sham et al., 1993; Schneider-Maunoury et al., 1993; Nonchev et al., 1996a,b; Vesque et al., 1996; Theil et al., 1998), and directly or indirectly the expression of *Hoxb3* in r5 and *follistatin* in r3 (Seitanidou et al., 1997). kreisler is a direct regulator of *Hoxb-3* in r5 (Manzanares et al., 1997). Interestingly, in these two latter cases, a hierarchic relationship is established between segmentation genes and genes possibly involved in specification of positional information or lineage restriction. In contrast to the significant progress made in unravelling the regulatory cascades, the identification of putative redundant or synergistic functions has lagged behind, a consequence of the lack of availability of double loss-of-function mutants affecting these genes. Recently, genetic analysis of double mutants has shown that *Hoxa1* and *Hoxb1* synergize in the early specification of r4 identity and in patterning r4-derived structures and neural crest (Gavalas et al., 1998; Studer et al., 1998). In addition, the establishment of *Hoxb1* expression in r4 depends on the early activation of both *Hoxa1* and *Hoxb1* by endogenous retinoids (Dupé et al., 1997; Studer et al., 1998).

In the present work, we have investigated the possible synergy between *Krox-20* and *Hoxa1*. During hindbrain development, *Krox-20*, which encodes a zinc finger transcription factor (Chavrier et al., 1988, 1990), is successively activated in two transverse stripes that prefigure and subsequently coincide with r3 and r5 (Wilkinson et al., 1989a; Schneider-Maunoury et al., 1993). As indicated above, Krox-20 is required for the maintenance of the r3 and r5 territories (Schneider-Maunoury et al., 1993, 1997; Swiatek and Gridley, 1993). *Hoxa1* presents a very dynamic pattern of expression in the neuroectoderm. By the headfold stage, it reaches a sharp anterior limit corresponding to the prospective r3/r4 boundary, and later on this expression regresses caudally (Lufkin et al., 1991; Murphy and Hill, 1991; Dupé et al., 1997). The *Hoxa1* loss-of-function mutation, in addition to its dramatic effect on r4 and r5 mentioned above, was also shown to result in an increase in the size of r3 (Carpenter et al., 1993; Dollé et al., 1993; Gavalas et al., 1998). Since *Hoxa1* has not been observed to be expressed rostrally to the prospective r3/r4 boundary, such a phenotype was unexpected and suggested a non-autonomous effect of the mutation on r3. We have investigated this possibility in further detail and observed additional modifications in r3 following inactivation of *Hoxa1*. In particular, these abnormalities include the appearance of territories of r2-like identity within this rhombomere as well as additional features normally characteristic of even-numbered rhombomeres. In addition, we have found that these phenotypes become more severe when one allele of *Krox-20* is inactivated. Our data therefore suggest that the development of r3 is non-autonomous and that *Krox-20* and *Hoxa1* synergize in its patterning.

## MATERIALS AND METHODS

### Mouse lines and genotyping

The different mouse lines were maintained in a mixed C57Bl6/DBA2 background. Double heterozygous males and females were generated by mating heterozygous *Hoxa1* mutant mice (Lufkin et al., 1991) with heterozygous *Krox-20/lacZ* mutant mice (Schneider-Maunoury et al., 1993). Embryos carrying different combinations of the two mutations were obtained by crossing double heterozygous males with $Hoxa1^{+/-}$ females (or reverse). PCR genotyping of embryo yolk sac or mouse tail DNAs was performed as described (Schneider-Maunoury et al., 1993) for the *Krox-20* locus and with the following combination of three oligonucleotides for the *Hoxa1* locus: a common 3′ oligonucleotide in the *Hoxa1*-coding sequence (5′ CATGGGAGTCGAGAGGTTTC-CAGAG 3′) and two 5′ oligonucleotides located in the *Hoxa1* 5′ flanking region (5′ GCCATTGGCTGGTAGAGTCACGTGT 3′) and in the $neo^R$-coding sequence (5′ GATGGAAGCCGGTCTTGTCGAT-CAG 3′), respectively. These latter oligonucleotides give rise to PCR products of different sizes with the wild-type and mutant alleles of the *Hoxa1* gene respectively. PCR was performed as described previously (Schneider-Maunoury et al., 1993). The *EphA4/lacZ* and *r2-HPAP* transgenic lines were obtained by injection of previously described constructs containing the *lacZ*-coding sequence under the control of 8.5 kb of *EphA4* 5′ flanking genomic sequences (Theil et al., 1998) and the human placental alkaline phosphatase gene under the control of an *Hoxa2* enhancer element (Studer et al., 1996), respectively. Transgenic *EphA4/lacZ* or *r2-HPAP* males were bred with $Hoxa1^{+/-}$ females to produce $Hoxa1^{+/-}$ *EphA4/lacZ* and $Hoxa1^{+/-}$ *r2-HPAP* animals. The latter were crossed with $Hoxa1^{+/-}$ or $Hoxa1^{+/-}$ $Krox\text{-}20^{+/-}$ animals to produce the adequate embryos carrying the transgene. Detection of the presence of the transgenes was performed by PCR as previously described (Studer et al., 1996; Theil et al., 1998).

### X-gal and alkaline phosphatase staining and estimation of the areas corresponding to *lacZ*-positive or -negative cells within r3

X-gal staining was performed on whole-mount embryos as previously described (Schneider-Maunoury et al., 1993). Embryos were then washed in PBS, fixed overnight in 4% paraformaldehyde (PFA) in PBS and washed again in PBS. The neural tube was dissected by removing mesodermal tissues, opened along the dorsal midline for stages corresponding to a closed tube and flat mounted in glycerol. The areas of each half rhombomere 3 and of the patches of *lacZ*-positive and -negative cells were estimated by application of the computer programme neurolab (Microvision Instruments) on camera-lucida drawings. In $Hoxa1^{-/-}$ *EphA4/lacZ* and $Hoxa1^{-/-}$ $Krox\text{-}20^{+/-}$ embryos, r3 anterior and posterior boundaries were defined on each side of the flat-mounted embryo in a way that the total area included the most anterior and posterior *lacZ*-positive cells likely to belong to r3. Each *lacZ*-negative patch in this r3 domain was delimited and the corresponding areas were added to obtain the surface of *lacZ*-negative regions within r3. A precise estimation of the areas of the patches could not be obtained at 8.5 dpc. For alkaline phosphatase (AP) detection, the embryos were heated at 70°C in PBS for 90 minutes to inactivate the endogenous enzyme, after X-gal staining if required. AP activity was revealed as described for whole-mount in situ hybridisation.

### Immunocytochemistry and whole-mount in situ hybridisation

For immunocytochemistry or whole-mount in situ hybridisation, the embryos were either fixed directly in PFA overnight at 4°C or processed for X-gal staining before overnight fixation in PFA. Immunocytochemistry on dissected neural tubes was performed as described by Schneider-Maunoury et al. (1993). The 2H3 monoclonal antibody and the anti-EphA4 polyclonal antibody (Becker et al., 1995) were used at final dilutions of 1:5000 and 1:20000, respectively. For 2H3 staining, a horseradish peroxidase (HRP)-conjugated goat anti-mouse secondary antibody (Sigma) was used and revealed with diaminobenzidine. For anti-EphA4 staining, an alkaline-phosphatase (AP)-conjugated goat anti-rabbit antibody (Sigma) was used and revealed with NBT-BCIP (Boehringer). Whole-mount in situ

hybridisation was performed as described by Prince and Lumsden (1994). The RNA probes included an 800 bp *Pst*I-*Apa*I fragment from the *Krox-20* cDNA (Wilkinson et al., 1989a), an 800 bp *Eco*RI fragment from the mouse *Hoxb1* cDNA (Wilkinson et al., 1989b), a 1.2 kb fragment (positions 652-1834) from the *EphA4* cDNA (Gilardi-Hebenstreit et al., 1992), an 860 bp *Taq*I fragment from the *Hoxa2* gene, and a 3 kb *Eco*RI-*Not*I fragment from the *Hoxb2* gene (Wilkinson et al., 1989b).

## RESULTS

### Hoxa1 function is required for normal r3 development

To analyse the effect of the *Hoxa1* mutation on r3 development, we first used *Krox-20* as a marker since it is expressed at a high level in this rhombomere from approximately the 0 somite stage to the 18-somite stage (Fig. 1A, Wilkinson et al., 1989a; Schneider-Maunoury et al., 1993). As expected, in 8.5 day post coitum (dpc) *Hoxa1*$^{-/-}$ embryos, expression of *Krox-20* in the hindbrain was mainly restricted to a single band, previously identified as r3 according to its rostrocaudal position and relative location with respect to other rhombomeric markers (Fig. 1B,D; Lufkin et al., 1991; Chisaka et al., 1992; Carpenter et al., 1993; Dollé et al., 1993; Mark et al., 1993). The loss-of-function allele of *Hoxa1* used in this study leads to a dramatic reduction of r5 (Lufkin et al., 1991; Dollé et al., 1993; Mark et al., 1993). Consistently, a few small patches of *Krox-20*-expressing cells were also observed more caudally, corresponding to remnants of r5 (Fig. 1B,D). The distance between r3 and these r5 remnants was less than a rhombomere width, reflecting a partial loss of r4 in *Hoxa1*$^{-/-}$ embryos (Lufkin et al., 1991; Chisaka et al., 1992; Carpenter et al., 1993; Dollé et al., 1993; Mark et al., 1993). Although *Hoxa1* is not expressed in the presumptive r3 territory, the r3 *Krox-20*-positive stripe in *Hoxa1*$^{-/-}$ embryos presented two abnormal features: its rostrocaudal width was significantly enlarged as compared to wild-type embryos (Fig. 1, see also Carpenter et al., 1993; Gavalas et al., 1998) and it was not homogeneous; small patches of *Krox-20*-negative cells were observed within the stripe (Fig. 1B,D). This preliminary analysis indicated that lack of Hoxa1 affects the normal development of r3.

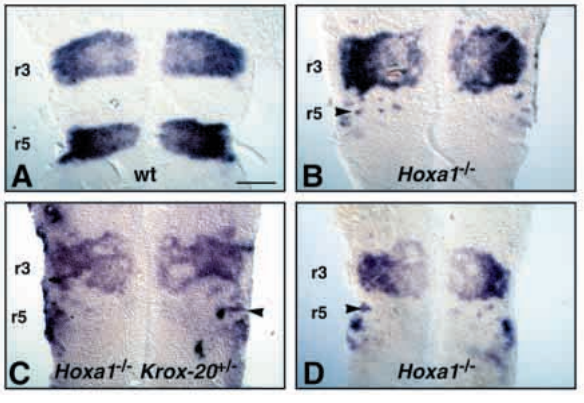


**Fig. 1.** r3 development is affected by the *Hoxa1* loss-of-function mutation. Flat-mounted hindbrains were prepared from whole-mount 8.5 dpc embryos (8 to 16 somites) hybridised with a *Krox-20* probe. (A) Wild-type, (B,D) *Hoxa1*$^{-/-}$, (C) *Hoxa1*$^{-/-}$ *Krox-20*$^{+/-}$ embryos. In *Hoxa1*$^{-/-}$ and double mutants embryos, r3 is enlarged and contains patches of *Krox-20*-negative cells. Remnants of r5 are indicated by arrowheads. Scale bar, 100 μm.

### The *Hoxa1*$^{-/-}$ phenotype in r3 is affected by the *Krox-20* mutation in a dosage-dependent manner

To investigate a possible effect of a reduction of the level of *Krox-20* on the r3 phenotype in *Hoxa1* mutant embryos, we combined the two mutations. In *Hoxa1*$^{+/-}$ *Krox-20*$^{+/-}$ embryos, no modification of the *Krox-20* expression pattern was observed as compared to wild-type embryos (data not shown). In *Hoxa1*$^{-/-}$ *Krox-20*$^{+/-}$ embryos, as in the case of the *Hoxa1*$^{-/-}$ embryos, r3 was enlarged as compared to the wild-type situation (Fig. 1A,C). In addition, similar numbers of *Krox-20*-negative patches were observed in r3, although their size appeared larger than in *Hoxa1*$^{-/-}$ embryos (Fig. 1). To analyse the r3 phenotype in further detail, we made use of two *lacZ* reporters to follow *Krox-20* expression more easily. The *Krox-20* mutation used in these experiments involves an in-frame insertion of the *lacZ* sequence within the *Krox-20* gene, giving rise to a hybrid gene. The activity of the Krox-20/β-galactosidase fusion protein has been shown to recapitulate *Krox-20* expression (Fig. 2J,K; Schneider-Maunoury et al., 1993, 1997; Topilko et al., 1994; Levi et al., 1996; Murphy et al., 1996). The second *lacZ* reporter was introduced by crossing with a transgenic line in which the *lacZ* gene has been placed under the control of the *EphA4* gene promoter with 8.5 kb of 5′ flanking sequence (Theil et al., 1998). This region includes a *Krox-20*-dependent *cis*-acting element, which places the transgene under the direct transcriptional control of Krox-20 (Theil et al., 1998). In this transgenic line, *lacZ* expression in the hindbrain is restricted to r3 and r5 (Fig. 2A,B).

At 8.5 dpc, in *Hoxa1*$^{-/-}$ embryos carrying the *EphA4/lacZ* transgene or in *Hoxa1*$^{-/-}$ *Krox-20*$^{+/-}$ embryos, detection of β-galactosidase activity by X-gal staining revealed that r3 was enlarged about 2-fold and contained *lacZ*-negative patches (Fig. 2D,G). These patches are likely to correspond to the *Krox-20*-negative patches observed by in situ hybridisation. They were in similar number (around 11 per half rhombomere) in the two genotypes. At this stage, the small size of the patches prevented a quantitative comparison of their cumulated areas in *Hoxa1*$^{-/-}$ and *Hoxa1*$^{-/-}$ *Krox-20*$^{+/-}$ embryos.

The higher stability of the β-galactosidase as compared to the *Krox-20* mRNA allowed the study of the maintenance of the patches at a later stage of development (9.5 dpc), when *Krox-20* has started to be downregulated in r3 (Fig. 2B,E,H,K; Schneider-Maunoury et al., 1993; Theil et al., 1998). To allow quantitative analysis of the areas covered by the *lacZ*-negative patches, camera-lucida drawings of r3 territories were performed (Fig. 2C,F,I,L). In both genotypes, the number of patches was around 4 per half rhombomere, a number significantly reduced from its estimation at 8.5 dpc. Two striking differences were observed between the two genotypes. (i) The cumulated area of the *lacZ*-negative patches represented a much larger part of the rhombomere in *Hoxa1*$^{-/-}$ *Krox-20*$^{+/-}$ embryos (28.5%) than in *Hoxa1*$^{-/-}$ embryos (7.9%) (Fig. 2M). This high proportion of *lacZ*-negative cells in *Hoxa1*$^{-/-}$ *Krox-20*$^{+/-}$ embryos led to highly disordered stripes and made it sometimes difficult to define r3 boundaries (Fig. 2H,I). (ii) While patches were mainly located within the basal plate in both genotypes, the percentage of the area of the patches

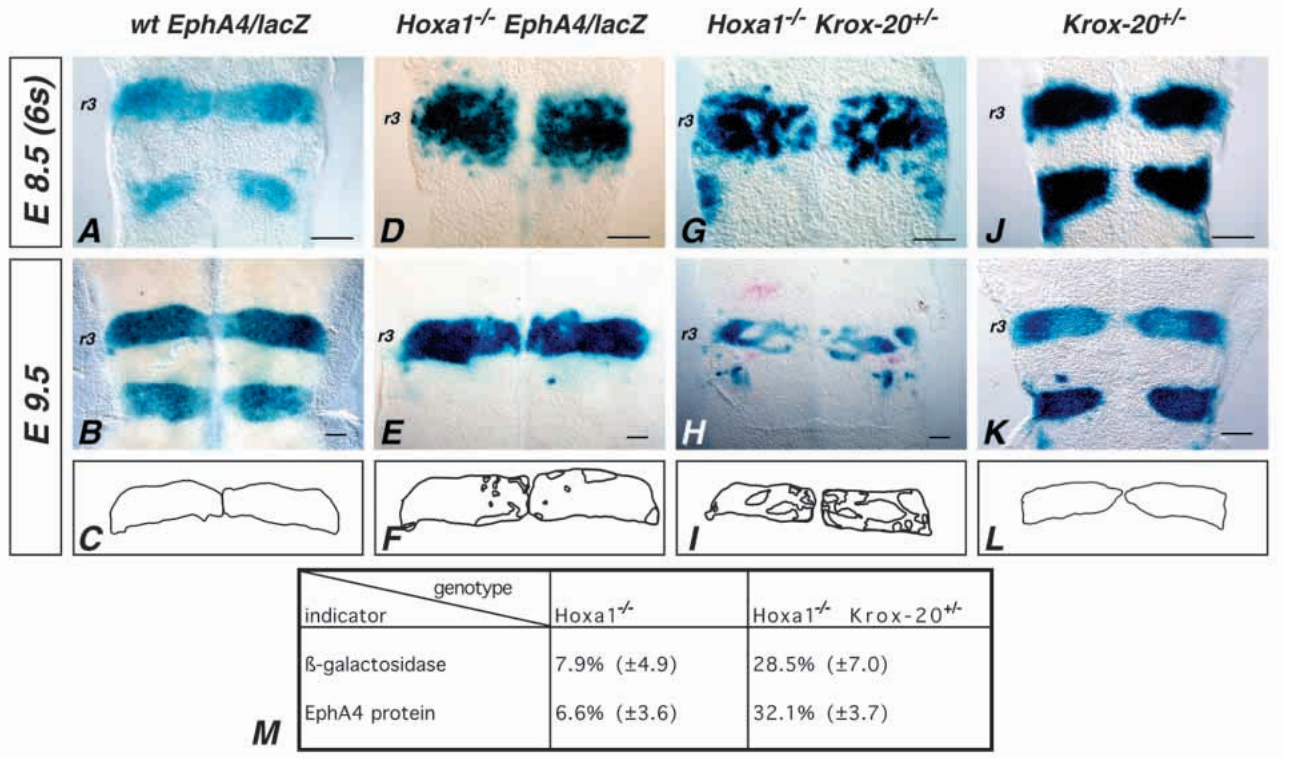


**Fig. 2.** *Krox-20* and *Hoxa1* synergize for r3 development. Flat mounts of 8.5 dpc (A,D,G,J) or 9.5 dpc (B,E,H,K) embryo hindbrains analysed by X-gal staining to reveal the β-galactosidase activity due to the *EphA4/lacZ* transgene (A,B,D,E) or the *Krox-20/lacZ* knock-in (G,H,J,K). The genotypes of the embryos are as follow: (A,B) *EphA4/lacZ*, (D,E) *Hoxa1*$^{-/-}$ *EphA4/lacZ*, (G,H) *Hoxa1*$^{-/-}$ *Krox-20*$^{+/-}$, (J,K) *Krox-20*$^{+/-}$. (C,F,I,L) The boundaries between X-gal-positive and -negative regions as well as the presumptive limits of r3 corresponding to (B,E,H,K) have been drawn using a camera lucida. (M) The proportion of the r3 area occupied by non-r3 patches was estimated from the comparison of *lacZ*-negative and -positive or EphA4 low- and high-level territories. In *EphA4/lacZ* and *Krox-20*$^{+/-}$ embryos, both at 8.5 and 9.5 dpc, X-gal staining reveals two homogeneous stripes corresponding to r3 and r5, respectively. At 8.5 dpc, *Hoxa1*$^{-/-}$ *EphA4/lacZ* and *Hoxa1*$^{-/-}$ *Krox-20*$^{+/-}$ embryos present an enlarged r3 with a high number of small *lacZ*-negative patches. At 9.5 dpc, the *lacZ*-negative patches occupy a much larger part of r3 in *Hoxa1*$^{-/-}$ *Krox-20*$^{+/-}$ than in *Hoxa1*$^{-/-}$ *EphA4/lacZ* embryos. Scale bars, 100 μm.

located in the dorsal part of the rhombomere was 7.5% in the case of *Hoxa1*$^{-/-}$ embryos versus 20% in the case of double mutants (data not shown).

In conclusion, these data have confirmed the existence of *Krox-20*-negative patches within r3 from *Hoxa1*$^{-/-}$ embryos at 8.5 dpc and have established their persistence during subsequent development. In addition, they indicate that the inactivation of one allele of the *Krox-20* gene results in an about 3-fold increase in the area of r3 occupied by the patches in the *Hoxa1*$^{-/-}$ background, at least at the 9.5 dpc stage. This latter point has been confirmed by analysis of another marker, identical for the two genotypes. As will be discussed below, the levels of EphA4 mRNA and protein are reduced in the *lacZ*-negative patches. Quantitative analysis of the areas of the patches of reduced EphA4 protein level within r3 led to a conclusion identical to the study of the X-gal-negative patches, i.e. a significant increase is observed when one allele of *Krox-20* is inactivated (Fig. 2M). Our data therefore suggest that *Hoxa1* and *Krox-20* synergize for the establishment of the integrity of r3 and that this effect is dependent on the dosage of *Krox-20*.

### The *Krox-20*-negative patches in r3 present an r2-like molecular identity

The existence of patches of *Krox-20*-negative cells in r3 is likely to reflect the disturbance of important early events occurring during normal hindbrain development. Understanding the identity and origin of these cells might provide important insights in the molecular mechanisms controlling this process. Each rhombomere can be characterised by the expression of a specific combination of marker genes, which reflects the molecular identity of the corresponding cells (for a review, see Lumsden and Krumlauf, 1996). To analyse the molecular identity of the cells in the *Krox-20*-negative patches, we first performed in situ hybridisations with several rhombomere-specific probes. At around 9.5 dpc, *Hoxb1* constitutes a specific marker of r4 (Fig. 3A; Murphy et al., 1989; Wilkinson et al., 1989b) and *Hoxb2* expression is restricted to the part of the central nervous system (CNS) caudal to the r2/r3 boundary, with high relative levels in r3, r4 and r5 (Fig. 3E; Wilkinson et al. 1989b; Sham et al., 1993); *Hoxa2* and *EphA4* are expressed at high relative levels in r3 and r5 and at lower levels in r2, r4 and caudally to r5 in the case of *Hoxa2* (Fig. 3I; Nonchev et al., 1996a; Frasch et al., 1995), and in r2, r4 and r6 in the case of *EphA4* (Fig. 3M; Gilardi-Hebenstreit et al., 1992; Nieto et al., 1992). In *Hoxa1*$^{-/-}$ embryos, the domain of expression of *Hoxb1* was dramatically reduced (Fig. 3B), reflecting the loss of part of r4 as previously reported (Lufkin et al., 1991; Chisaka et al., 1992; Carpenter et al., 1993; Dollé et al., 1993; Mark et al., 1993). The situation was similar in *Hoxa1*$^{-/-}$ *Krox-20*$^{+/-}$ embryos (Fig.

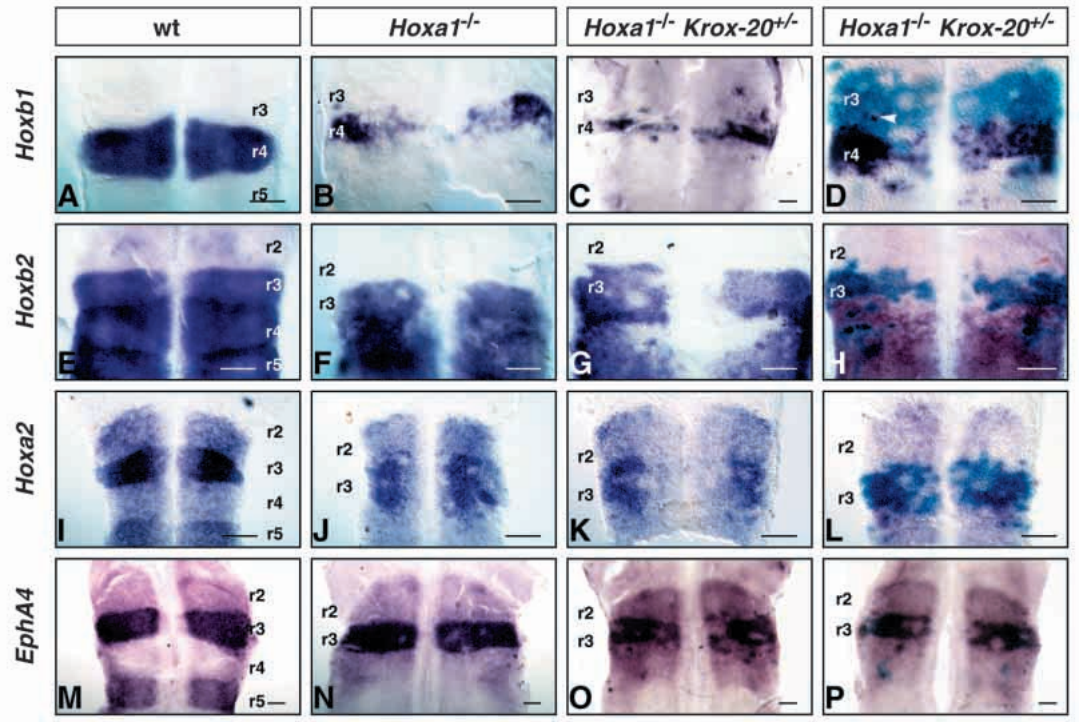


**Fig. 3.** The *Krox-20*-negative patches in r3 express an r2-like combination of markers. The expression of *Hoxb1* (A-D), *Hoxb2* (E-H), *Hoxa2* (I-L) and *EphA4* (M-P) was analysed by whole-mount in situ hybridisation in 9-9.5 dpc embryos. Flat-mounted hindbrains from wild-type (A,E,I,M), *Hoxa1*$^{-/-}$ (B,F,J,N) and *Hoxa1*$^{-/-}$ *Krox-20*$^{+/-}$ (C,D,G,H,K,L,O,P) embryos are shown. In addition, in half of the *Hoxa1*$^{-/-}$ *Krox-20*$^{+/-}$ embryos, β-galactosidase activity was revealed by X-gal staining to visualise *lacZ*-positive and -negative regions in r3 (D,H,L,P). In wild-type embryos, *Hoxb1* marked specifically r4 (A), *Hoxb2* mRNA was found exclusively posterior to the r2/r3 boundary (E), *Hoxa2* (I) and *EphA4* (M) expression levels were high in r3 and r5, and lower in r2, r4 and r6. In both *Hoxa1*$^{-/-}$ and *Hoxa1*$^{-/-}$ *Krox-20*$^{+/-}$ embryos, *Hoxb1* mRNA was rarely found rostral to the remnants of r4 (B-D). Double labelling with X-gal (D) indicated that the *lacZ*-negative patches did not express *Hoxb1*, except for a few cells occasionally (arrowhead). Patches of *Hoxb2*-negative cells (F-H) or of cells expressing low levels of *Hoxa2* (J-L) or *EphA4* (N-P) were observed in r3 in *Hoxa1*$^{-/-}$ or *Hoxa1*$^{-/-}$ *Krox-20*$^{+/-}$ embryos. Double labelling indicated that most cells in the X-gal-negative patches did not express *Hoxb2* and expressed low levels of *Hoxa2* and *EphA4* (H,L,P). Note that in both *Hoxa1*$^{-/-}$ and *Hoxa1*$^{-/-}$ *Krox-20*$^{+/-}$ embryos, *Hoxb1*- and *Hoxb2*-negative cells were often observed in the ventral-most part of r4 as well (B-D and F-H, respectively). The hybridisation probes are indicated on the left. Scale bars, 100 μm.

3C) and double labelling with X-gal indicated that most of the cells in the *lacZ*-negative patches did not express *Hoxb1* (Fig. 3D). *Hoxb2*-negative patches were observed within r3 in both *Hoxa1*$^{-/-}$ and *Hoxa1*$^{-/-}$ *Krox-20*$^{+/-}$ embryos, the area of the patches being larger with the latter genotype as in the case of the *Krox-20*-negative patches (Fig. 2F,G). Double labelling with X-gal in *Hoxa1*$^{-/-}$ *Krox-20*$^{+/-}$ embryos demonstrated that most of the cells from the *Krox-20*-negative patches did not express *Hoxb2* either (Fig. 3H). Finally, in the case of both *Hoxa2* and *EphA4*, in *Hoxa1*$^{-/-}$ and *Hoxa1*$^{-/-}$*Krox-20*$^{+/-}$ embryos, patches of cells were observed within the r3 domain where their expression levels were lower than those in the surrounding r3 and more similar to those observed in r2/r4 (Fig. 3J-L,N-P). Double-labelling experiments in *Hoxa1*$^{-/-}$ *Krox-20*$^{+/-}$ embryos indicated that the r3 *lacZ*-negative patches expressed low levels of *Hoxa2* or *EphA4* (Fig. 3L,P).

Taken together, these data indicate that within the *Krox-20*-negative patches most of the cells do not express either *Hoxb1* or *Hoxb2* and express *Hoxa2* and *EphA4* at levels lower than in normal r3, similar to those of r2/r4. Such a combination of specific levels of gene expression is clearly different from that normally present in r3, r4 and r5. This combination is identical to that of r2, raising the possibility that the *Krox-20*-negative patches in r3 have an r2 identity. To address this possibility more directly, we made use of a transgenic line, r2-HPAP, which expresses specifically the human placental alkaline phosphatase (AP) gene in r2 (Studer et al., 1996; Fig. 4A). Introduction of the transgene in *Hoxa1*$^{-/-}$ and *Hoxa1*$^{-/-}$ *Krox-20*$^{+/-}$ backgrounds revealed that: (i) in both types of embryos, r3 contains patches of AP-positive cells (Fig. 4B-D), and (ii) most of the *lacZ*-negative patches in *Hoxa1*$^{-/-}$ *Krox-20*$^{+/-}$ embryos are AP-positive (Fig. 4C,D). Nevertheless, occasionally, *lacZ*- and AP-negative patches were observed within r3 (Fig. 4C). In any case, the r2-HPAP analysis is in agreement with the study of the other regional markers and indicates that most of the *lacZ*-negative patches have an r2-like molecular identity. Finally, it is also interesting to note that, in *Hoxa1*$^{-/-}$ and *Hoxa1*$^{-/-}$ *Krox-20*$^{+/-}$ embryos, an r2-like pattern of gene expression is also often seen within the ventral-most part of r4 (Figs 3B-D,F-H, 4B,D), similar to that observed in *Hoxb1* mutant embryos (Studer et al., 1996). This suggests that the *Hoxa1* mutation may differentially affect r4 development along its dorsoventral axis. Nevertheless, a morphological boundary is observed between r3 and r4, as in wild-type embryos (data not shown).

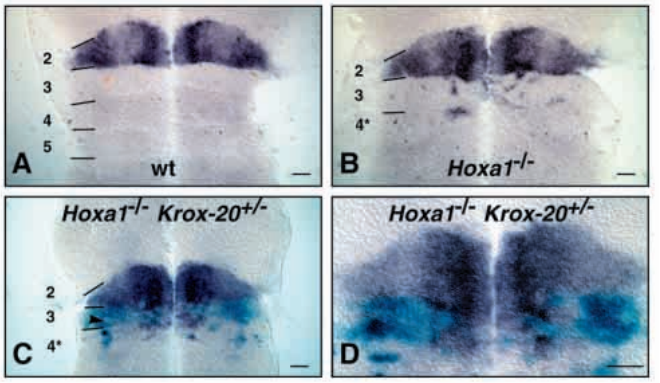


**Fig. 4.** The *Krox-20*-negative patches in r3 express an r2-specific transgene. Flat-mounted hindbrains from wild-type (A), *Hoxa1*$^{-/-}$ (B) and *Hoxa1*$^{-/-}$ *Krox-20*$^{+/-}$ (C,D) 9.5 dpc embryos carrying the *r2-HPAP* transgene were stained for alkaline phosphatase (AP) activity. (C,D) β-galactosidase activity was also revealed to visualise *Krox-20*-positive and -negative territories in r3. While AP activity is confined to r2 in wild-type embryos, patches of AP-positive cells are observed caudal to r2 in *Hoxa1*$^{-/-}$ embryos. In *Hoxa1*$^{-/-}$ *Krox-20*$^{+/-}$ embryos, larger AP-positive patches are observed within r3, where they correspond to the *lacZ*-negative territories. Occasionally, patches are observed which are negative for both *lacZ* and AP (arrowhead in C). r4* represents the fused rhombomere including remnants of r4, r5 and r6.

## r3 neuronal differentiation is affected in *Hoxa1*$^{-/-}$ embryos

Neuronal differentiation within each rhombomere is known to reflect its even- or odd-number character. To further investigate the properties and the fate of r3 in *Hoxa1*$^{-/-}$ and *Hoxa1*$^{-/-}$ *Krox-20*$^{+/-}$ embryos, we analysed neuronal differentiation by immunostaining with an antibody, 2H3, directed against the $155\times10^3$ $M_r$ component of neurofilaments, which allows labelling of both cell bodies and axons. In addition, the embryos were double-labelled by X-gal staining or with an anti-EphA4 antibody in order to identify territories of r3 identity (the developing was kept minimal to avoid masking the neurons). In wild-type embryos, motor neurons differentiate in the vicinity of the floor plate, extending their axons ipsilaterally away from the midline. Their differentiation begins at around the 19-somite stage in even-numbered rhombomeres and at around the 25-somite stage in odd-numbered rhombomeres (Fig. 5A,B and data not shown). Therefore, at the 24-somite stage r2 and r4 are rich in neurons, whereas r3 is still almost completely devoid of motor neurons (Fig. 5B). In *Hoxa1*$^{-/-}$ 21-somite embryos, motoneurons are normally present in r2 and in the remnants of r4 (Fig. 5D). In addition, neuronal differentiation has clearly been initiated in r3 as well. However, the r3 motor-like neurons are located slightly more ventrally than the motor column in adjacent even-numbered rhombomeres. This atypical location of r3 motor-like neurons in *Hoxa1*$^{-/-}$ embryos was clearer at the 24-somite stage (Fig. 5E). In *Hoxa1*$^{-/-}$ *Krox-20*$^{+/-}$ embryos, r3 neuronal differentiation appeared even more advanced than in *Hoxa1*$^{-/-}$ embryos and similar to that in the adjacent even-numbered rhombomeres (Fig. 5G,H). In this case, the dorsoventral location of the motor neurons was identical to that in even-numbered rhombomeres.

In conclusion, in *Hoxa1*$^{-/-}$ embryos, neurogenesis takes place earlier than normal in r3, at the same time as in the even-numbered rhombomeres (Fig. 5C,F). Nevertheless, neuronal differentiation appears less intense in r3 than in adjacent even-numbered rhombomeres. In addition, the early r3 putative motor neurons are located more ventrally than the motor column in even-numbered rhombomeres. In *Hoxa1*$^{-/-}$ *Krox-20*$^{+/-}$ embryos, early r3 neurons are generated in higher number than in *Hoxa-1*$^{-/-}$ embryos and the motor neurons are located

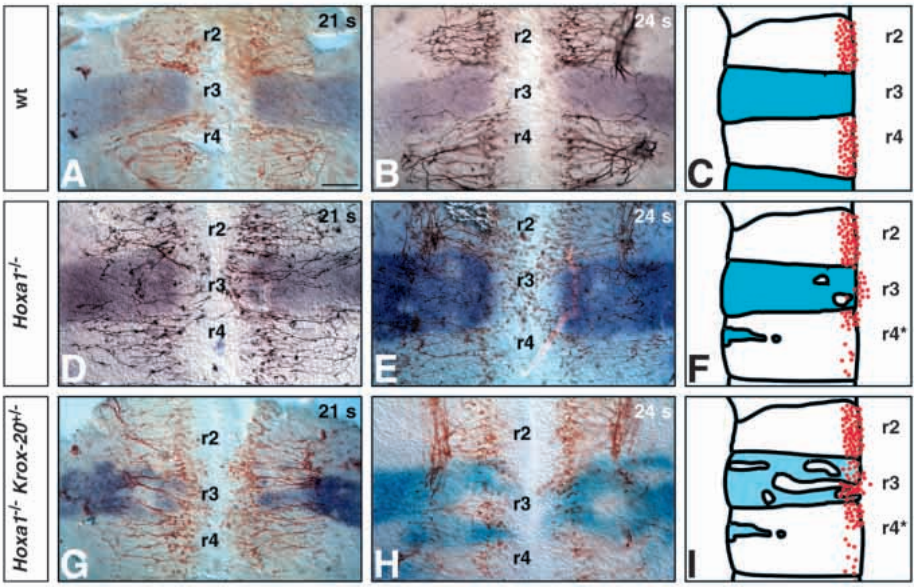


**Fig. 5.** Analysis of r3 neurogenesis in 9.5 dpc wild-type and mutant embryos. Flat-mounted hindbrains of 21-somite (A,D,G) and 24-somite (B,E,H) wild-type (A,B), *Hoxa1*$^{-/-}$ (D,E) and *Hoxa1*$^{-/-}$ *Krox-20*$^{+/-}$ (G,H) embryos were stained with the 2H3 anti-neurofilament antibody. This was combined with an anti-EphA4 antibody labelling (A,B,D,E,G) or with X-gal staining (H) to reveal regions of r3 identity. In a wild-type 21-somite embryo (A), only r2 and r4 contain motor neurons, whereas in a slightly older embryo (24 somites, B), a few neurons are visible in r3. Note longitudinal axons at the alar/basal boundary extending to the level of r2 or r3. In *Hoxa1*$^{-/-}$ embryos, motor-like neurons are present in r3 from the 21-somite stage (D). They are located slightly more ventrally than the motor neurons in even-numbered rhombomeres. In 24-somite *Hoxa1*$^{-/-}$ embryos (E), these early motor-like r3 neurons have accumulated and are still located more ventrally than the motor column. In *Hoxa1*$^{-/-}$ *Krox-20*$^{+/-}$ embryos (G,H), motor neuron differentiation in r3 occurs more extensively than in *Hoxa1*$^{-/-}$ embryos. These neurons are located in a dorsoventral position similar to that of the motor neurons in the adjacent even-numbered rhombomeres. Scale bar, 100 μm. (C,F,I) Schematic representation of the r3 phenotypes. The domains of *Krox-20* expression are figured in blue and the intensity of the colour reflects the number of functional alleles. Patches of *Krox-20*-negative cells are observed in *Hoxa1*$^{-/-}$ embryos. These patches are larger and more dorsal in *Hoxa1*$^{-/-}$ *Krox-20*$^{+/-}$ embryos. The differentiated motor neurons are figured by red dots.

at the same dorsoventral level as in even-numbered rhombomeres (Fig. 5I). Therefore, the motor column of *Hoxa1*$^{-/-}$ *Krox-20*$^{+/-}$ embryos appears continuous, with no visible difference between r3 and the adjacent even-numbered rhombomeres. It is possible that the difference in ventrodorsal location of the motor neurons between *Hoxa1*$^{-/-}$ and *Hoxa1*$^{-/-}$ *Krox-20*$^{+/-}$ embryos is related to the difference in extent of the territories with r3 identity or with a normal dosage of *Krox-20* within the r3 basal plate (Figs 2, 5), which might repel early differentiating neurons.

### Abnormal navigation of r3 motor axons

The segmental pattern of neurogenesis in the hindbrain prefigures the metameric organisation of branchiomotor nerves, which involves a co-operation between pairs of adjacent rhombomeres. In particular, the trigeminal (V) and facial (VII) nerves have their exit points located in r2 and r4, respectively, and receive axonal contributions from motor neurons born in r1/r2/r3 and in r4/r5 (Marshall et al., 1992; Carpenter et al., 1993). Using retrograde motor neuron tracing, Gavalas and collaborators have shown that, in *Hoxa1*$^{-/-}$ embryos, r3 hosts a variable population of motor neurons projecting towards the facial ganglion through multiple and ectopic r3 exit points (Gavalas et al., 1998). We have performed similar experiments by anterograde labelling with DiI and reached identical conclusions (data not shown). In *Hoxa1*$^{-/-}$ *Krox-20*$^{+/-}$ embryos, the abnormal navigation phenotype of r3 motor neurons appeared more severe, but was still variable (data not shown).

In order to perform a more extensive analysis of this phenomenon, we studied the presence of ectopic r3 motor roots by a combination of neurofilament and EphA4 (to visualise r3) immunochemistry. In wild-type embryos, the trigeminal and facial motor nerve exit points are separated by a rhombomere width corresponding to r3 and the two nerves remain separated and innervate branchial arches 1 and 2, respectively (Fig. 6A). With mutant embryos, we observed a wide variety of phenotypes that were grouped into five categories according to their severity (Fig. 6): the mildest phenotype involves the appearance of a unique, thin, ectopic rootlet within r3 (Fig. 6B), while the most severe is characterised by the presence of large ectopic roots all along r3, combined with a fusion of the Vth and VIIth nerves, which project into the second branchial arch (Fig. 6H). The distribution of half-embryos of a particular genotype within these categories revealed the following points (Fig. 6I): (i) while *Hoxa1*$^{+/-}$ embryos were essentially of the wild-type character, half of the *Krox-20*$^{+/-}$ embryos presented a minor phenotype and a few a more severe one, (ii) the combination of the *Hoxa1* and *Krox-20* mutations led to significant increases in the severity of the phenotype, both in *Hoxa1* heterozygous or homozygous states, and (iii) severe phenotypes can be observed despite the presence of an apparently normal r4, in the case of double heterozygous embryos (Fig. 6D).

In conclusion, these data indicate that the mutations inactivating *Hoxa1* and *Krox-20* affect r3 neuronal navigation in a synergistic and dose-dependent manner for both genes. They also suggest that this phenotype is not directly related to the strong reduction of r4 and to the development of patches of r2-like identity within r3 since these two manifestations are never observed in *Hoxa1*$^{+/-}$ *Krox-20*$^{+/-}$ embryos (data not shown). An important question is whether the change in navigation is intrinsic or extrinsic to r3 motor neurons. We

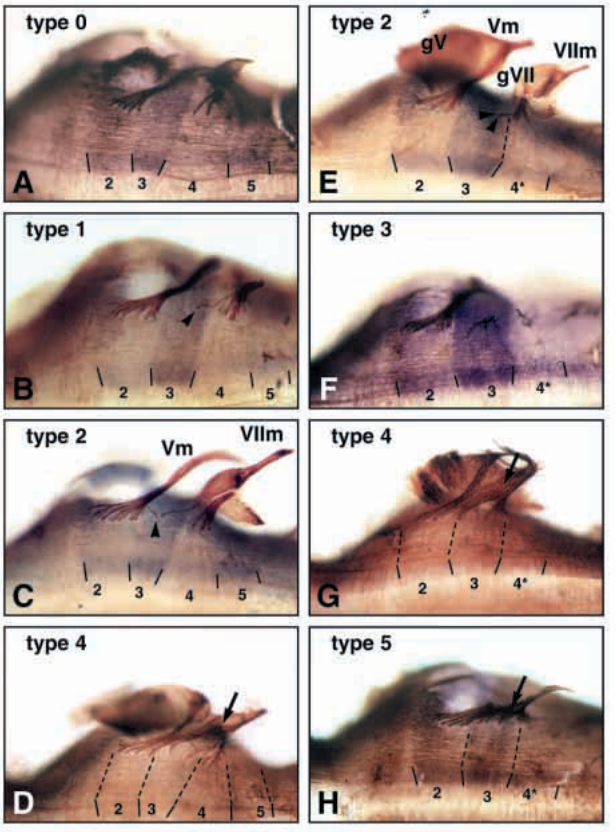


I

| n | genotype | 0 | 1 | 2 | 3 | 4 | 5 |
|---|---|---|---|---|---|---|---|
| 30 | wt | 100% | | | | | |
| 64 | *Hoxa1*$^{+/-}$ | 80% | 20% | | | | |
| 28 | *Krox-20*$^{+/-}$ | 46% | 43% | 4% | 7% | | |
| 63 | *Hoxa1*$^{+/-}$ *Krox-20* $^{+/-}$ | 27% | 27% | 19% | 16% | 11% | |
| 41 | *Hoxa1*$^{-/-}$ | 10% | 14% | 20% | 44% | 12% | |
| 35 | *Hoxa1*$^{-/-}$ *Krox-20*$^{+/-}$ | 3% | 8.5% | 8.5% | 51.5% | 20% | 8.5% |

**Fig. 6.** Analysis of nerves V and VII motor roots reveals a dosage-dependent synergism between *Krox-20* and *Hoxa1*. (A-H) Ventral views of 10.5 dpc dissected neural tubes (right side) immunostained with the 2H3 anti-neurofilament antibody alone (D,G) or in combination with an anti-EphA4 antibody as a marker of r3 (A-C,E,F,H). The genotypes of the embryos are wild type (A), *Hoxa1*$^{+/-}$ *Krox-20*$^{+/-}$ (B,C,D), *Hoxa1*$^{-/-}$ (E,F) and *Hoxa1*$^{-/-}$ *Krox-20*$^{+/-}$ (G,H). Note that in A-D r4 and r5 are present. The embryos have been grouped into six categories (0 to 5) according to the absence or the severity of the phenotype affecting the motor roots. Type 0, no ectopic root in r3 (A); type 1, one ectopic root (arrowhead in B); type 2, two ectopic roots joining Vm and VIIm (C, arrowhead) or VIIm (E, arrowheads); type 3, multiple ectopic roots in r3 (F); type 4, combination of multiple ectopic roots in r3 with defasciculation of axons from Vm and rerouting to VIIm (G, arrow); type 5, combination of ectopic roots all along r3 and fusion of Vm and VIIm toward the second branchial arch (H, arrow). (I) The frequency of the phenotypic categories (0-5) for each genotype. n, number of cases; Vm, trigeminal motor nerve; VIIm, facial motor nerve; gV, trigeminal ganglion; gVII, facial ganglion. Rhombomeres are indicated.

favour the second possibility since *Krox-20*-expressing cells are observed at the level of the exit points in r3 (data not shown). This suggest the presence of ectopic boundary cap cells at the level of r3. These cells, derived from the neural crest, are thought to be involved in guiding migratory motor axons towards the exit points (Wilkinson et al., 1989a;

Niederlander and Lumsden, 1996) and they are normally restricted to even-numbered rhombomeres. In mutant embryos, ectopic boundary cap cells in r3 may override the chemoattractive signals from the r2 exit point and lead to the generation of exit points in r3.

## DISCUSSION

In this study, we have established the implication of *Hoxa1* in the control of the development of r3. In absence of the *Hoxa1* gene product, r3 contains patches of cells with an r2-like molecular identity and shows even-numbered rhombomere characters both in terms of neuronal differentiation and axonal navigation. This phenomenon was unexpected since *Hoxa1* has not been observed to be expressed rostrally to the prospective r3/r4 boundary. Furthermore, we discovered a genetic synergy between *Hoxa1* and *Krox-20* in the patterning of r3 since the additional inactivation of one allele of *Krox-20* led to more severe phenotypes in r3. These different phenotypic manifestations suggest novel functions for *Hoxa1* and *Krox-20*.

### Non-autonomous r3 development

Our data indicate that the inactivation of *Hoxa1* results in two early phenotypes in r3: the rhombomere width is increased at early stages (8.5 dpc) and patches of cells presenting an r2-like identity are observed within the rhombomere. The domain of transcription of *Hoxa1* has never been observed rostrally to the r3/r4 prospective boundary, although it is not possible to exclude that *Hoxa1* is expressed transiently in the prospective r3 region at a very early stage, before the onset of *Krox-20* expression (Murphy and Hill, 1991; Lufkin et al., 1991; Alexandre et al., 1996; Dupé et al., 1997). Therefore, the available data suggest that the inactivation of *Hoxa1* interferes with a signal extrinsic to r3 and required for the normal development of this rhombomere. The transient expression of *Hoxa1* in the adjacent prospective rhombomere 4 makes this latter rhombomere a good candidate for the source of such a signal. Since the *Hoxa1* mutation leads to a partial elimination of r4, two non-exclusive possibilities can be envisaged to explain the contribution of *Hoxa1* in r3 development: (i) *Hoxa1* controls the generation of the r4 signal required for r3 normal development and/or (ii) it is the reduction in size of r4 that leads to a decrease in signalling towards r3. In this latter case, the effect of the *Hoxa1* mutation on r3 is only indirect and *Hoxa1* does not formally control r3 development.

Other manifestations of a non-autonomous control of r3 development have been reported previously. The transplantation of r3 into the r4 position in the chick leads to the downregulation of *Krox-20* and *Msx-2* expression as well as ectopic crest production in both donor and recipient r3 (Graham et al., 1993; Graham and Lumsden, 1996). In collagen gel culture assays, r3 was able to maintain *Krox-20* expression only when cultured together with r4 (Graham et al., 1994). Our data, therefore, extend these observations and demonstrate that exogenous signal(s), possibly originating from r4, play an essential role in the determination of r3 identity, as demonstrated by the presence of the patches and by the abnormal r3 neuronal specification occurring in the *Hoxa1* mutant.

### Dosage-dependent synergy between *Krox-20* and *Hoxa1*

The inactivation of one allele of the *Krox-20* gene in a wild-type background does not lead to the appearance of any defect apart from the mild r3 navigation phenotype described above (Fig. 6; Schneider-Maunoury et al., 1993, 1997; Swiatek and Gridley, 1993). In contrast, when associated with the inactivation of *Hoxa1*, it reinforces three of the *Hoxa1* r3 phenotypes and leads to the disappearance of a fourth manifestation of this mutation (Fig. 5C,F,I). (i) In the $Hoxa1^{-/-}$ $Krox\text{-}20^{+/-}$ embryos, the total area of the *Krox-20*-negative patches in r3 was significantly increased at 9.5 dpc as compared to $Hoxa1^{-/-}$ embryos. (ii) The early differentiation of part of the r3 neuronal population observed in $Hoxa1^{-/-}$ embryos was extended to a larger population in $Hoxa1^{-/-}$ $Krox\text{-}20^{+/-}$ embryos so that the number of neurons in r3 was similar to that in even-numbered rhombomeres. (iii) The navigation phenotype of r3 axons is more severe in $Hoxa1^{-/-}$ $Krox\text{-}20^{+/-}$ embryos than in $Hoxa1^{-/-}$ embryos. The synergism between the two genes for this phenotype is also observed in double heterozygous embryos. (iv) In contrast, the abnormal ventral localisation of most of the early r3 motor-like neurons in $Hoxa1^{-/-}$ embryos is not observed when the dosage of *Krox-20* is reduced by a factor of two. These different data indicate the existence of interactions between *Krox-20* and components of the genetic cascade initiated by the *Hoxa1*-dependent signalling in r3. These interactions appear to be synergistic in the first three aspects and possibly antagonistic in the fourth. Interestingly, these interactions are revealed by the disruption of only one allele of *Krox-20* and are, therefore, dosage-dependent with respect to this latter gene.

### Identity and origin of the *Krox-20*-negative patches within r3

We have shown that the cells from the large majority of the *Krox-20*-negative patches in r3 express a combination of markers (taking also into account their relative levels) consistent with an r2 molecular identity. This interpretation is in agreement with two other observations: (i) the absence of apparent mixing of the *Krox-20*-negative cells with the *Krox-20*-positive ones reflects the behaviour of cells from even-numbered rhombomeres which do not mix efficiently with those from odd-numbered rhombomeres (Guthrie et al., 1993; Wizenmann and Lumsden, 1997), and (ii) the behaviour of the r3 motor neurons in terms of differentiation time resemble that of even-numbered rhombomere neurons. It is tempting to speculate that these early differentiating neurons might have originated from the patches of non-r3 identity in the ventral-most region of the neural plate. Nevertheless the examination of their distribution with respect to the patches did not allow us to establish such a proposal, possibly because of unrestricted migration of the neurons in the mantel layer following their differentiation.

The reduction in the number of *Krox-20*-negative patches with time in $Hoxa1^{-/-}$ $Krox\text{-}20^{+/-}$ embryos suggests that they occasionally fuse with each other. However this cannot explain their increase in size between 8.5 and 9.5 dpc. This latter observation suggests that the r2-like identity is stably inherited during cell proliferation and that the patches constitute the clonal progeny of a few cells. This raises important issues about the involvement of *Hoxa1* and *Krox-20* in the generation of these early r2-like progenitors within r3 and/or in the expansion of the derived patches. We envisage three non-exclusive possibilities

where Hoxa1 acts at increasingly later stages in the development of the patches. (i) The *Krox-20*-negative patches are derived from r3 progenitors which once expressed *Krox-20* and switched to an r2-like identity. Hoxa1 function would be required to prevent this early identity switch of r3 cells. (ii) The patches are derived from *Krox-20*-negative, invading cells originating from r2 or r4, or from cells located within the prospective r3 territory, but which failed to activate *Krox-20* at early stage of r3 development. Such cells are present in the wild-type embryos as suggested by the non-homogeneous pattern of *Krox-20* expression in prospective r3 at the 0- to 4-somite stages (Irving et al., 1996). In this case, the *Hoxa1* mutation may interfere with a putative process which, by differential adhesion, change of identity or induction of apoptosis in response to a community effect, is responsible for the early segregation of *Krox-20*-positive and -negative cells (Wilkinson, 1995; Rijli et al., 1998; Schneider-Maunoury et al., 1998). (iii) According to the third hypothesis, a signal originating from r4 or dependent on Hoxa1 function would prevent the proliferation of the early *Krox-20*-negative cells present in prospective r3. One of the roles of *Krox-20* would be to counteract this signal in an autonomous manner and allow normal proliferation. Therefore, in wild-type embryos, the *Krox-20*-positive cells would largely outcompete the negative ones in r3. In *Hoxa1*$^{-/-}$ embryos, a large part of r4 being eliminated, the *Krox-20*-negative cells in r3 would be allowed to proliferate, although more slowly than the *Krox-20*-positive cells, resulting in small patches. In *Hoxa1*$^{-/-}$ *Krox-20*$^{+/-}$ embryos, the reduction of *Krox-20* dosage in the *Krox-20*-positive cells might slightly reduce their rate of proliferation, modifying the balance of the competition between *Krox-20*-positive and -negative cells and allowing the generation of larger patches of negative cells.

We favour this latter model because it is consistent with the phenotype of the *Krox-20*$^{-/-}$ embryos (Schneider-Maunoury et al., 1993; Swiatek and Gridley, 1993) and it provides a simple explanation for the apparent non-autonomous effect of the *Krox-20* mutation on the expansion of *Krox-20*-negative patches. In addition, a major advantage of such a complex mode of control of cell proliferation in r3 would be to make sure that the cells that will populate the rhombomere adjacent to r4 express *Krox-20* as well as its regional identity and segregation target genes (Seitanidou et al., 1997; Schneider-Maunoury et al., 1998). In this respect, this mechanism would link proximity to r4, cell proliferation, specification of identity and cell segregation through the multiple functions of Krox-20. It is interesting to note that, according to this model, despite the apparent synergy of the *Hoxa1* and *Krox-20* mutations for the impairment of r3 development, these genes have actually antagonistic effects at the cellular level, since a signal controlled by *Hoxa1* prevents cell proliferation while expression of *Krox-20* allows to escape this negative control in an autonomous manner. Finally, an important question for the future will be to determine which gene(s) among the direct transcriptional targets of Krox-20, such as *Hoxa2* and *Hoxb2*, are responsible for the genetic interaction with *Hoxa1*. It will therefore be interesting to combine mutant alleles of these genes with the *Hoxa1* loss-of-function mutation.

We thank Dr S. Schneider-Maunoury for valuable discussions all along this work, Dr R. Krumlauf for the *Hoxb1* and *Hoxb2* probes, Drs M. Studer and R. Krumlauf for the gift of the r2-HPAP construct, Dr M. Wassef for critical reading of the manuscript, and F. Laval and S. Hiard for excellent technical assistance. The 2H3 monoclonal antibody was obtained from the Developmental Studies Hybridoma Bank. Work in the Charnay laboratory was supported by grants from INSERM, MENRT, EEC, ARC and LNCC. Work in the Chambon laboratory was supported by funds from the INSERM, CNRS, UPL, Collège de France, ARC, FRM and LNCC. C. P. was supported by postdoctoral fellowships from the Human Frontier Science Programme and the European Union (TRM).

## REFERENCES

**Alexandre, D., Clarke, J. D., Oxtoby, E., Yan, Y. L., Jowett, T. and Holder, N.** (1996). Ectopic expression of Hoxa-1 in the zebrafish alters the fate of the mandibular arch neural crest and phenocopies a retinoic acid-induced phenotype. *Development* **122**, 735-746.

**Becker, N., Gilardi-Hebenstreit, P., Seitanidou, T., Wilkinson, D. and Charnay, P.** (1995). Characterisation of the Sek-1 receptor tyrosine kinase. *Febs Letters* **368**, 353-357.

**Birgbauer, E. and Fraser, S. E.** (1994). Violation of cell lineage restriction compartments in the chick hindbrain. *Development* **120**, 1347-1356.

**Birgbauer, E., Sechrist, J., Bronner-Fraser, M. and Fraser, S.** (1995). Rhombomeric origin and rostrocaudal reassortment of neural crest cells revealed by intravital microscopy. *Development* **121**, 935-945.

**Carpenter, E. M., Goddard, J. M., Chisaka, O., Manley, N. R. and Capecchi, M. R.** (1993). Loss of Hox-A1 (Hox-1.6) function results in the reorganization of the murine hindbrain. *Development* **118**, 1063-1075.

**Chavrier, P., Vesque, C., Galliot, B., Vigneron, M., Dolle, P., Duboule, D. and Charnay, P.** (1990). The segment-specific gene Krox-20 encodes a transcription factor with binding sites in the promoter region of the Hox-1.4 gene. *EMBO J.* **9**, 1209-1218.

**Chavrier, P., Zerial, M., Lemaire, P., Almendral, J., Bravo, R. and Charnay, P.** (1988). A gene encoding a protein with zinc fingers is activated during G0/G1 transition in cultured cells. *EMBO J.* **7**, 29-35.

**Chisaka, O., Musci, T. S. and Capecchi, M. R.** (1992). Developmental defects of the ear, cranial nerves and hindbrain resulting from targeted disruption of the mouse homeobox gene Hox-1.6. *Nature* **355**, 516-520.

**Clarke, J. D. and Lumsden, A.** (1993). Segmental repetition of neuronal phenotype sets in the chick embryo hindbrain. *Development* **118**, 151-162.

**Cordes, S. P. and Barsh, G. S.** (1994). The mouse segmentation gene kr encodes a novel basic domain-leucine zipper transcription factor. *Cell* **79**, 1025-1034.

**Dollé, P., Lufkin, T., Krumlauf, R., Mark, M., Duboule, D. and Chambon, P.** (1993). Local alterations of Krox-20 and Hox gene expression in the hindbrain suggest lack of rhombomeres 4 and 5 in homozygote null Hoxa-1 (Hox-1.6) mutant embryos. *Proc. Natl. Acad. Sci. USA* **90**, 7666-7670.

**Dupé, V., Davenne, M., Brocard, J., Dollé, P., Mark, M., Dierich, A., Chambon, P. and Rijli, F. M.** (1997). In vivo functional analysis of the Hoxa-1 3′ retinoic acid response element (3′RARE). *Development* **124**, 399-410.

**Frasch, M., Chen, X. and Lufin, T.** (1995). Evolutionary-conserved enhancers direct region-specific expression of murine Hoxa-1 and Hoxa-2 loci in both mice and Drosophila. *Development* **121**, 957-974.

**Fraser, S., Keynes, R. and Lumsden, A.** (1990). Segmentation in the chick embryo hindbrain is defined by cell lineage restrictions. *Nature* **344**, 431-435.

**Frohman, M. A., Martin, G. R., Cordes, S. P., Halamek, L. P. and Barsh, G. S.** (1993). Altered rhombomere-specific gene expression and hyoid bone differentiation in the mouse segmentation mutant, kreisler (kr). *Development* **117**, 925-936.

**Gavalas, A., Davenne, M., Lumsden, A., Chambon, P. and Rijli, F. M.** (1997). Role of Hoxa-2 in axon pathfinding and rostral hindbrain patterning. *Development* **124**, 3693-3702.

**Gavalas, A., Studer, M., Lumsden, A., Rijli, F. M., Krumlauf, R. and Chambon, P.** (1998). *Hoxa1* and *Hoxb1* synergize in patterning the hindbrain, cranial nerves and second pharyngeal arch. *Development*, **125**, 1123-1136.

**Gilardi-Hebenstreit, P., Nieto, M. A., Frain, M., Mattei, M. G., Chestier, A., Wilkinson, D. G. and Charnay, P.** (1992). An Eph-related receptor protein tyrosine kinase gene segmentally expressed in the developing mouse hindbrain. *Oncogene* **7**, 2499-2506.

**Gould, A., Morrison, A., Sproat, G., White, R. A. and Krumlauf, R.** (1997). Positive cross-regulation and enhancer sharing: two mechanisms for specifying overlapping Hox expression patterns. *Genes Dev.* **11**, 900-913.

**Graham, A., Heyman, I. and Lumsden, A.** (1993). Even-numbered

rhombomeres control the apoptotic elimination of neural crest cells from odd-numbered rhombomeres in the chick hindbrain. *Development* **119**, 233-245.

**Graham, A., Francis-West, P., Brickell, P. and Lumsden, A.** (1994). The signalling molecule BMP4 mediates apoptosis in the rhombencephalic neural crest. *Nature* **372**, 684-686.

**Graham, A. and Lumsden, A.** (1996). Interactions between rhombomeres modulate Krox-20 and follistatin expression in the chick embryo hindbrain. *Development* **122**, 473-480.

**Guthrie, S., Prince, V. and Lumsden, A.** (1993). Selective dispersal of avian rhombomere cells in orthotopic and heterotopic grafts. *Development* **118**, 527-538.

**Irving, C., Nieto, A., DasGupta, R., Charnay, P. and Wilkinson, D.G**. (1996). Progressive spatial restriction of *Sek-1* and *Krox-20* gene expression during hindbrain segmentation. *Dev. Biol.*, **173**, 26-38.

**Kontges, G. and Lumsden, A.** (1996). Rhombencephalic neural crest segmentation is preserved throughout craniofacial ontogeny. *Development* **122**, 3229-3242.

**Levi, G., Topilko, P., Schneider-Maunoury, S., Lasagna, M., Mantero, S., Cancedda, R. and Charnay, P.** (1996). Defective bone formation in Krox-20 mutant mice. *Development* **122**, 113-120.

**Lufkin, T., Dierich, A., LeMeur, M., Mark, M. and Chambon, P.** (1991). Disruption of the Hox-1.6 homeobox gene results in defects in a region corresponding to its rostral domain of expression. *Cell* **66**, 1105-1119.

**Lumsden, A. and Guthrie, S.** (1991). Alternating patterns of cell surface properties and neural crest cell migration during segmentation of the chick hindbrain. *Development* **2**, 9-15.

**Lumsden, A. and Keynes, R.** (1989). Segmental patterns of neuronal development in the chick hindbrain. *Nature* **337**, 424-428.

**Lumsden, A. and Krumlauf, R.** (1996). Patterning the vertebrate neuraxis. *Science* **274**, 1109-1115.

**Lumsden, A., Sprawson, N. and Graham, A.** (1991). Segmental origin and migration of neural crest cells in the hindbrain region of the chick embryo. *Development* **113**, 1281-1291.

**Maconochie, M. K., Nonchev, S., Studer, M., Chan, S. K., Popperl, H., Sham, M. H., Mann, R. S. and Krumlauf, R.** (1997). Cross-regulation in the mouse HoxB complex: the expression of Hoxb2 in rhombomere 4 is regulated by Hoxb1. *Genes Dev.* **11**, 1885-1895.

**Manzanares, M., Cordes, S., Kwan, C. T., Sham, M. H., Barsh, G. S. and Krumlauf, R.** (1997). Segmental regulation of Hoxb-3 by kreisler. *Nature* **387**, 191-195.

**Mark, M., Lufkin, T., Vonesch, J. L., Ruberte, E., Olivo, J. C., Dolle, P., Gorry, P., Lumsden, A. and Chambon, P.** (1993). Two rhombomeres are altered in Hoxa-1 mutant mice. *Development* **119**, 319-338.

**Marshall, H., Nonchev, S., Sham, M. H., Muchamore, I., Lumsden, A. and Krumlauf, R.** (1992). Retinoic acid alters hindbrain Hox code and induces transformation of rhombomeres 2/3 into a 4/5 identity. *Nature* **360**, 737-741.

**McKay, I. J., Muchamore, I., Krumlauf, R., Maden, M., Lumsden, A. and Lewis, J.** (1994). The kreisler mouse: a hindbrain segmentation mutant that lacks two rhombomeres. *Development* **120**, 2199-2211.

**Murphy, P. and Hill, R. E.** (1991). Expression of the mouse labial-like homeobox-containing genes, Hox 2.9 and Hox 1.6, during segmentation of the hindbrain. *Development* **111**, 61-74.

**Murphy, P., Davidson, D. R. and Hill, R. E.** (1989). Segment-specific expression of a homoeobox-containing gene in the mouse hindbrain. *Nature* **341**, 156-159.

**Murphy, P., Topilko, P., Schneider-Maunoury, S., Seitanidou, T., Baron-Van Evercooren, A. and Charnay, P.** (1996). The regulation of Krox-20 expression reveals important steps in the control of peripheral glial cell development. *Development* **122**, 2847-2857.

**Niederlander, C. and Lumsden, A.** (1996). Late emigrating neural crest cells migrate specifically to the exit points of cranial branchiomotor nerves. *Development* **122**, 2367-2374.

**Nieto, M. A., Gilardi-Hebenstreit, P., Charnay, P. and Wilkinson, D. G.** (1992). A receptor protein tyrosine kinase implicated in the segmental patterning of the hindbrain and mesoderm. *Development* **116**, 1137-1150.

**Nonchev, S., Maconochie, M., Vesque, C., Aparicio, S., Ariza-McNaughton, L., Manzanares, M., Maruthainar, K., Kuroiwa, A., Brenner, S., Charnay, P. and Krumlauf, R.** (1996a). The conserved role of Krox-20 in directing Hox gene expression during vertebrate hindbrain segmentation. *Proc. Natl. Acad. Sci. USA* **93**, 9339-9345.

**Nonchev, S., Vesque, C., Maconochie, M., Seitanidou, T., Ariza-McNaughton, L., Frain, M., Marshall, H., Sham, M. H., Krumlauf, R. and Charnay, P.** (1996b). Segmental expression of Hoxa-2 in the hindbrain is directly regulated by Krox-20. *Development* **122**, 543-554.

**Popperl, H., Bienz, M., Studer, M., Chan, S. K., Aparicio, S., Brenner, S., Mann, R. S. and Krumlauf, R.** (1995). Segmental expression of Hoxb-1 is controlled by a highly conserved autoregulatory loop dependent upon exd/pbx. *Cell* **81**, 1031-1042.

**Prince, V. and Lumsden, A.** (1994). *Hoxa-2* expression in normal and transposed rhombomeres: independent regulation in the neural tube and neural crest. *Development* **120**, 911-923.

**Rijli, F. M., Gavalas, A. and Chambon, P.** (1998). Segmentation and specification in the branchial region of the head: the role of the *Hox* selector genes. *Int. J. Dev. Biol.* **42**, 393-401.

**Schneider-Maunoury, S., Seitanidou, T., Charnay, P. and Lumsden, A.** (1997). Segmental and neuronal architecture of the hindbrain of Krox-20 mouse mutants. *Development* **124**, 1215-1226.

**Schneider-Maunoury, S., Topilko, P., Seitandou, T., Levi, G., Cohen-Tannoudji, M., Pournin, S., Babinet, C. and Charnay, P.** (1993). Disruption of Krox-20 results in alteration of rhombomeres 3 and 5 in the developing hindbrain. *Cell* **75**, 1199-1214.

**Schneider-Maunoury, S., Gilardi-Hebenstreit, P. and Charnay, P.** (1998) How to build a vertebrate hindbrain: lessons from genetics. *C. R. Acad. Sci.*, in press.

**Seitanidou, T., Schneider-Maunoury, S., Desmarquet, C., Wilkinson, D. G. and Charnay, P.** (1997). Krox-20 is a key regulator of rhombomere-specific gene expression in the developing hindbrain. *Mech. Dev.* **65**, 31-42.

**Serbedzija, G. N., Bronner-Fraser, M. and Fraser, S. E.** (1992). Vital dye analysis of cranial neural crest cell migration in the mouse embryo. *Development* **116**, 297-307.

**Sham, M. H., Vesque, C., Nonchev, S., Marshall, H., Frain, M., Gupta, R. D., Whiting, J., Wilkinson, D., Charnay, P. and Krumlauf, R.** (1993). The zinc finger gene Krox20 regulates HoxB2 (Hox2.8) during hindbrain segmentation. *Cell* **72**, 183-196.

**Studer, M., Lumsden, A., Ariza-McNaughton, L., Bradley, A. and Krumlauf, R.** (1996). Altered segmental identity and abnormal migration of motor neurons in mice lacking Hoxb-1. *Nature* **384**, 630-634.

**Studer, M., Gavalas, A., Marshall, H., Ariza-McNaughton, L., Rijli, F. M., Chambon, P. and Krumlauf, R.** (1998). Genetic interactions between *Hoxa1* and *Hoxb1* reveal new roles in regulation of early hindbrain patterning. *Development*, **125**, 1025-1036.

**Swiatek, P. J. and Gridley, T.** (1993). Perinatal lethality and defects in hindbrain development in mice homozygous for a targeted mutation of the zinc finger gene Krox20. *Genes Dev.* **7**, 2071-2084.

**Theil, T., Frain, M., Gilardi-Hebenstreit, P., Flenniken, A., Charnay, P. and Wilkinson, D. G.** (1998). Segmental expression of the *EphA4* (*Sek-1*) receptor tyrosine kinase in the hindbrain is under transcriptional control of Krox-20. *Development*, **125**, 443-452.

**Topilko, P., Schneider-Maunoury, S., Levi, G., Baron-Van Evercooren, A., Chennoufi, A. B., Seitanidou, T., Babinet, C. and Charnay, P.** (1994). Krox-20 controls myelination in the peripheral nervous system. *Nature* **371**, 796-799.

**Vesque, C., Maconochie, M., Nonchev, S., Ariza-McNaughton, L., Kuroiwa, A., Charnay, P. and Krumlauf, R.** (1996). Hoxb-2 transcriptional activation in rhombomeres 3 and 5 requires an evolutionarily conserved cis-acting element in addition to the Krox-20 binding site. *EMBO J.* **15**, 5383-5396.

**Wilkinson, D. G.** (1995). Genetic control of segmentation in the vertebrate hindbrain. *Perspect Dev. Neurobiol.* **3**, 29-38.

**Wilkinson, D. G., Bhatt, S., Chavrier, P., Bravo, R. and Charnay, P.** (1989a). Segment-specific expression of a zinc-finger gene in the developing nervous system of the mouse. *Nature* **337**, 461-464.

**Wilkinson, D. G., Bhatt, S., Cook, M., Boncinelli, E. and Krumlauf, R.** (1989b). Segmental expression of Hox-2 homoeobox-containing genes in the developing mouse hindbrain. *Nature* **341**, 405-409.

**Wingate, R. J. and Lumsden, A.** (1996). Persistence of rhombomeric organisation in the postsegmental hindbrain. *Development* **122**, 2143-2152.

**Wizenmann, A. and Lumsden, A.** (1997). Segregation of rhombomeres by differential chemoaffinity. *Mol. Cell Neurosci.* **9**, 448-459.

**Xu, Q., Alldus, G., Holder, N. and Wilkinson, D. G.** (1995). Expression of truncated Sek-1 receptor tyrosine kinase disrupts the segmental restriction of gene expression in the Xenopus and zebrafish hindbrain. *Development* **121**, 4005-4016.

**Zhang, M., Kim, H. J., Marshall, H., Gendron-Maguire, M., Lucas, D. A., Baron, A., Gudas, L. J., Gridley, T., Krumlauf, R. and Grippo, J. F.** (1994). Ectopic Hoxa-1 induces rhombomere transformation in mouse hindbrain. *Development* **120**, 2431-2442.